Journal Pre-proof

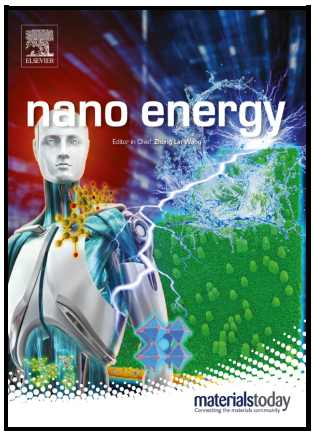

High-throughput Identification of Highly Active and Selective Single-Atom Catalysts for Electrochemical Ammonia Synthesis through Nitrate Reduction

Shuo Wang, Haixing Gao, Lei Li, Kwan San Hui, Duc Anh Dinh, Shuxing Wu, Sachin Kumar, Fuming Chen, Zongping Shao, Kwun Nam Hui

PII: S2211-2855(22)00594-8

DOI: https://doi.org/10.1016/j.nanoen.2022.107517

Reference: NANOEN107517

To appear in: *Nano Energy*

Please cite this article as: Shuo Wang, Haixing Gao, Lei Li, Kwan San Hui, Duc Anh Dinh, Shuxing Wu, Sachin Kumar, Fuming Chen, Zongping Shao and Kwun Nam Hui, High-throughput Identification of Highly Active and Selective Single-Atom Catalysts for Electrochemical Ammonia Synthesis through Nitrate Reduction, *Nano Energy,* () doi:https://doi.org/10.1016/j.nanoen.2022.107517

This is a PDF file of an article that has undergone enhancements after acceptance, such as the addition of a cover page and metadata, and formatting for readability, but it is not yet the definitive version of record. This version will undergo additional copyediting, typesetting and review before it is published in its final form, but we are providing this version to give early visibility of the article. Please note that, during the production process, errors may be discovered which could affect the content, and all legal disclaimers that apply to the journal pertain.

© Published by Elsevier.

Journal Pre-proof

High-throughput Identification of Highly Active and Selective Single-Atom Catalysts for Electrochemical Ammonia Synthesis through Nitrate Reduction

Shuo Wang[a,#], Haixing Gao[a,#], Lei Li[b,*], Kwan San Hui[c,*], Duc Anh Dinh[d], Shuxing Wu[e], Sachin Kumar[f], Fuming Chen[g], Zongping Shao[h,i,*], Kwun Nam Hui[a,*]

[a] Joint Key Laboratory of the Ministry of Education, Institute of Applied Physics and Materials Engineering, University of Macau, Avenida da Universidade, Taipa, Macau SAR, P.R. China. Email: bizhui@um.edu.mo

[b] Hefei National Laboratory for Physical Sciences at the Microscale, Collaborative Innovation Center of Chemistry for Energy Materials, University of Science and Technology of China, Hefei 230026, P.R. China. Email: uestclilei@163.com

[c] School of Engineering, Faculty of Science, University of East Anglia, Norwich, NR4 7TJ, United Kingdom. Email: k.hui@uea.ac.uk

[d] NTT Hi-Tech Institute, Nguyen Tat Thanh university, Ho Chi Minh city 700000, Vietnam

[e] Guangzhou Key Laboratory of Clean Transportation Energy Chemistry, School of Chemical Engineering and Light Industry, Guangdong University of Technology, Guangzhou 510006, P.R. China.

[f] School of Chemical Engineering, Yeungnam University, Gyeongsan, Gyeongbuk 38541, Republic of Korea.

[g] State Key Laboratory of Optic Information Physics and Technologies, School of Physics and Telecommunication Engineering, South China Normal University, Guangzhou 510006, P.R. China

[h] State Key Laboratory of Materials-Oriented Chemical Engineering, College of Chemical Engineering, Nanjing Tech University, Nanjing 211816, P.R. China. E-mail: shaozp@njtech.edu.cn

[i] WA School of Mines: Minerals, Energy and Chemical Engineering (WASM-MECE), Curtin 21 University, Perth, WA 6102, Australia.

[#] These authors contribute equally.

Abstract

The highly selective and active nitrate-to-ammonia electrochemical conversion (NO_3 reduction reaction [NO_3RR]) can be an appealing and supplementary alternative to the Haber-Bosch process. It also opens up a new idea for addressing nitrate pollution. Previous study

Journal Pre-proof

demonstrated that FeN_4 single-atom catalyst (SAC) indicates excellent NO_3RR performance. Nonetheless, the mechanism that triggers the electrocatalytic NO_3RR remains unclear. The feasibility of NO_3RR over various SACs is verified in this study via high-throughput density functional theory calculations with the single transition metal (TM) atom coordinated with four nitrogen atoms supported on graphene as the example. We conducted a comprehensive screening of TM SAC candidates for stability, NO_3^- adsorption strength, catalytic activity, and selectivity. Results reveal that the most promising candidate among the 23 TM SACs is Os SAC with a low limiting potential of −0.42 V. Os SAC is better than Fe SAC with a limiting potential of −0.53 V because of the strong interaction between the oxygen of NO_3^- species and Os atom. The origin of high NO_3RR activity of Os SAC is explained by its inner electronic structure of the strong hybridization of the Os atom and NO_3^- caused by the increasing charge transfer from TM atom to NO_3^-, leading to the suitable NO_3^- adsorption. This research provides a fundamental insight of discovering novel NO_3RR catalysts and may provide a motivating drive for the creation of effective ammonia electrocatalysts for further experimental investigation.

Key words: high-throughput calculations, single-atom catalysts, nitrate reduction, ammonia synthesis, electrocatalysis

Journal Pre-proof

Introduction

The discharge of domestic sewage has increased sharply with the development of industries and agriculture and the continuous growth of the population. The concentration of nitrate (NO_3^-) in drinking water has been rising, causing major pollution of water resources, serious harm to human health, and terrible diseases, such as cancer and blue baby syndrome.[1,]

[2] The removal of nitrate pollution in broad groundwater areas is a global issue because of the excellent stability of nitrate under normal aerobic conditions. According to the principle of remediation, the current treatment methods for a small part of groundwater nitrate pollution are divided into three categories: physical and chemical remediation technology, bioremediation technology, and chemical reduction technology. However, cleaning huge areas of nitrate pollution from groundwater, which is still a longstanding and tedious task, is a global issue.[3] Finding an effective and environmentally friendly way to treat nitrate wastewater is critically required; thus, it has become a popular research issue.

Alternatively, electrochemical NO_3^- reduction reaction (NO_3RR) for ammonia (NH_3) synthesis is regarded as a potential strategy for converting NO_3^- based on electrochemical technologies to eliminate nitrate contaminants in wastewater.[4-7 8,9] In addition, NH_3 is one of the most fundamental chemical raw materials and an essential energy storage medium.[10-14] However, traditional industrial-scale synthesis of NH_3 still has many drawbacks, such as harsh reaction conditions requiring high temperature (400−500 °C) and high pressure (150−300 atm), and the use of traditional energy sources, such as coal, generates a large amount of CO_2 emissions; this scenario is not conducive to the sustainable development of energy and the environment.[15-18] Furthermore, the industrial targeted product of electrochemical methods to remove nitrate contaminants is mainly N_2, with NH_3 as the by-product.[19-22] In particular, NO_3RR provides a competitive route for ammonia (NH_3) synthesis by transferring nine protons and eight electrons ($NO_3^- + 9H^+ + 8e^- \rightarrow NH_3 + 3H_2O$), which is essential for low-temperature ammonia synthesis.[23,24] Thus, developing high-performance electrocatalysts to convert nitrate waste into value-added NH_3 selectively is a promising strategy for resolving energy and environmental issues. It will also pave the way for a new nitrate treatment method.

Journal Pre-proof

Compared with bulk or nanosized transition metal (TM) catalysts, single-atom catalysts (SACs) have sparked considerable research interest in the field of catalysis due to their highest atom usage efficiency and unique atomic structure and electronic characteristics.[25-27] In many catalytic reactions, SACs show outstanding advantages, such as excellent activity, exceptional selectivity, and high stability.[28-36] Recent studies also demonstrated that SACs exhibit excellent performance by anchoring on various substrates,[37-39] which can effectively avoid the problem of metal agglomeration. Among these, covalent organic frameworks (COFs) have been widely used in the design of various SAC electrocatalysts in recent years due to their tunable nanopore size, high accessible surface area, and predesigned building units, abundant active sites, designable chain structures, and programmable topologies.[40,41] Very recently, Zhang, Wang, and Liu, et al. reported that iron-phthalocyanine based COF (denoted as FePc-BBL COF) exhibits unusual oxygen reduction reaction (ORR) activities and fast kinetics with a remarkable half-wave potential of 0.933 V and an ultralow Tafel slope of 24.8 mV dec^{-1} in alkaline media. In addition, the FePc-BBL COF also exhibits outstanding zinc-air battery performance when employed as a cathode electrocatalyst.[42] Another work discovered that Co-N-C SAC of metalloporphyrin-based COF exhibits the highest catalytic activity for hydrogen peroxide synthesis with high faraday efficiency at 84%, a large turnover frequency of 9.05 s^{-1} per Co site, and productivity of 909 mmol g_{cat}^{-1} h^{-1}.[43]

NO_3RR on single-atom catalysts has increasingly been observed in recent years, and various investigations have been reported. The single-atom Cu catalyst was the first proposed TM SAC to reduce nitrate to ammonia considerably via experiment; the strong binding between Cu and N (particularly Cu-N_2) is the key to favorable adsorption of NO_3^- and NO_2^-.[44] Niu et al. systematically explored the selectivity and activity of a single TM

supported on carbon nitride in the reduction of nitrate to ammonia by performing first-principle calculations; they finally screened out Ti/g-CN and Zr/g-CN because of their strong adsorption of NO_3^-.[23] Lv et al. discussed the activity and selectivity of TM/g-C_3N_4 single-atom catalysts to the electrocatalytic reduction of nitrates to NH_3 by performing first-principle calculations.[45] Notably, there are still many other excellent works that reported different supporting materials for NO_3RR. For example, Zhao's group demonstrated that Os anchored on graphdiyne was identified as an ideal NO_3RR catalyst with a low limiting potential (-0.37 V) and great suppressing effect on the competing reactions by systematically evaluating the activity and selectivity of various candidates.[46] However, the development of graphitic alkyne in electrocatalysis is limited by its poor electrical conductivity and complex synthesis process. Last year, Li, Zhao and Yu et al. reported that In deposited on Pd nanoparticles shows room-temperature nitrate catalytic reduction activity and proves mechanistic of catalyst performance, but the NH_3 yield rate and Fradaic efficiency are still unsatisfactory.[47] Graphene, a single-layer two-dimensional carbon material with unique structural and electrical characteristics, has been found to offer excellent support for SACs. Recently, nitrogen-doped graphene supported Fe SAC has been experimentally reported recently as an active and selective electrical catalyst that can convert nitrates to valuable ammonia because of the lack of neighboring metal sites, which can effectively prevent the N-N coupling step required for N_2 and then promote ammonia product selectivity.[48] Despite the excellent activity and selectivity of SAC for the nitrate reduction to ammonia, research on this topic is still in its early stages. What are the primary variables that influence catalytic selectivity? Why do the activities of various SACs differ considerably? Experiments demonstrated that Fe SAC has excellent activity and selectivity. Hence, does another metal with performance superior to Fe performance exist? Appropriately analyzing the feasibility of

Journal Pre-proof

SACs on NO_3RR and revealing the specific mechanism of SACs are essential to answer the issues mentioned.

The NO_3RR performance of SACs is extensively examined first in this work by high-throughput first-principle computation using a single TM (from Ti to Au) supported on N-doped graphene-based catalysts (denoted as TM SAC), as shown in **Figure 1b**. A four-step screening method is considered, and the reaction mechanisms that convert NO_3^- to NH_3 are classified as O-end, O-side, N-end, N-side, and NO-dimer. A volcano map and NH_3 desorption energy are constructed to describe activity patterns on TM_{SA} SAC. Among the 23 proposed catalysts, Os SAC is a rather promising catalyst for the electrochemical NO_3RR to produce NH_3 with efficient activity and selectivity. The limiting potential of Os SAC for NO_3RR to NH_3 is 0.42 V, which is lower than the limiting potential of experimentally synthesized Fe SAC (0.52 V). Furthermore, the genesis of NO_3RR activity and the experimental feasibility of Fe SAC and Os SAC are investigated. Our work screens and designs more efficient NO_3RR catalyst based on the very mature Fe SAC catalyst and also decreases the time and economic cost of trial and error in the NO_3RR experimental study.

Results and discussion

Structure and stability of TM SAC

In recent years, SACs have attracted increasing interest and applications in the field of catalysis owing to their high activity and selectivity. The systems we choose to investigate are SACs supported by nitrogen-doped graphene, which have been extensively studied, realized through experiments, and applied to many catalysis fields.[49] Inspired by the recently synthesized Fe SAC catalyst to reduce NO_3^- to NH_3, we studied the catalytic performance of a series of TM SACs. As shown in **Figure 1a**, we employed a four-step screening method to confirm whether TM SAC is suitable for the reduction of nitrate to ammonia and marked the

criteria for each step of screening process in detail as shown in **Figure S1**. First, verifying that TM can be stably anchored into the carbon layer is necessary.[50] Second, NO_3^- can be stably adsorbed on the TM SAC, which is also a necessary criterion for the entire screening step and can ensure the subsequent reaction.[51] In particular, the adsorption energy of NO_3^- must be satisfied: $\Delta G_{*NO3} < 0$. Third, the catalyst activity screening, that is, the TM SAC with a large limiting potential (U_L, by calculating the Gibbs free energy), is eliminated. Finally, the selectivity of the remaining catalysts must be confirmed, which is achieved by calculating U_L, to ensure that the synthesis of NH_3 in the NO_3RR process has a lower U_L than that in other competitive reaction products (H_2, N_2, NO, and NO_2).[45,48] Subsequently, **Figure 1b** displays that the TM atom coordinated with four nitrogen atoms is joined in graphene to replace two C vacancies. A total of 23 composed systems of TMs are calculated in this work, and the optimized structures are displayed in **Figure S2** (Supporting Information). The geometric structure of TM SACs is retained well. However, some TMs with large radius are out of the plane after full structural relaxation. Furthermore, the thermodynamic stabilities of TM SAC candidates are examined by the binding energy E_b, which is defined as follows: $E_b = E_{TM\,SAC} - E_{N4C} - E_{TM}$, where $E_{TM\,SAC}$ and E_{N4C} represent the total energies of the TM SAC candidate and the pristine substrate, and E_{TM} is the energy of the isolated TM atom. As shown in **Figure S3**, our calculated values of E_b are all well below zero except for Ag SAC. This observation implies the high thermodynamic stability of most TM SAC candidates. Thus, the Ag atom is first ruled out.

NO_3 Adsorption on TM SAC

The initial step in the NO_3RR process is the adsorption of NO_3^-, which plays a key role in the whole catalytic reaction. Thus, the adsorption strength of NO_3^- on TM SAC must be determined. **Figure S4** depicts the consideration of two possible initial configurations of

Journal Pre-proof

NO_3^- adsorbed on TM centers (1-O and 2-O patterns). As shown in **Table S1**, NO_3^- prefers to adsorb on TM SAC via the 2-O pattern (two oxygen atoms adsorbed on TM SAC); the adsorption energy of the 2-O pattern is more negative than that of the 1-O pattern. Furthermore, the adsorption strength of NO_3^- on bare graphene is examined. From another perspective, the relatively weak NO_3^- adsorption (+1.56 eV) on bare graphene demonstrates the importance of TM active sites in NO_3RR activation. **Figure 1c** depicts the adsorption energies of NO_3^- (G_{*NO3}), H proton (G_{*H}), and N_2 molecule (G_{*N2}) on TM SAC. **Figure S5** depicts the corresponding configurations of *H and *N_2. The negative adsorption energy indicates that the NO_3^- adsorption to the TM SAC substrate is a spontaneous exothermic process, which is favorable to the subsequent reaction. On the contrary, if the adsorption energy is positive, then NO_3^- cannot be adsorbed on the substrate spontaneously, and follow-up reactions cannot be performed. Except for the TM SAC, including Co, Ni, Cu in 3d, Rh and Pd in 4d, and Ir, Pt, and Au in 5d, the majority of the TM SAC adsorptions of NO_3^- are an exothermic process, which proves to be an excellent potential catalyst. The ΔG^*_{NO3} values of most candidates are more negative than G_{*H} and G_{*N2} values on the TM SAC for the early TM SACs, suggesting that NO_3RR is favorable.

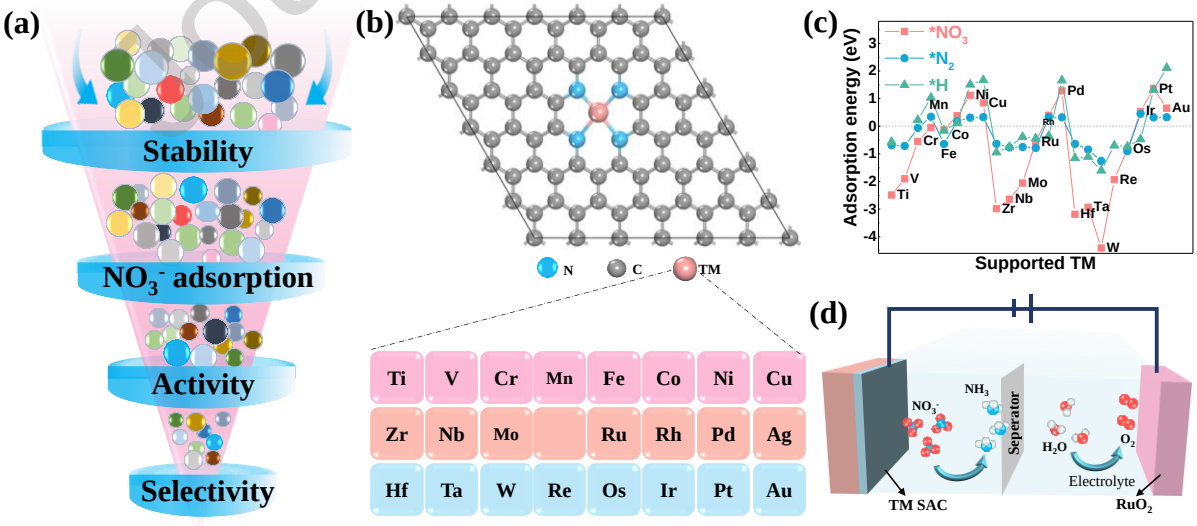

Figure 1. a) Schematic illustration of metals considered in this work for screening. b) Top view of the TM SAC atomic structure. Atom labels: C (grey), N (blue), and TM (pink). A list of the screened TM atoms (from Ti to Au) exists. c) Adsorption energies of NO_3^-, N_2 molecule, and H proton on TM SAC are compared. d) Schematic representation of the proposed electrochemical cell for NO_3RR (cathode: TM SAC) and Oxygen evolution reaction (OER) (anode: RuO_2, for example).

NO_3RR Mechanism on TM SAC

The electrochemical conversion of NO_3^- to NH_3 is a complicated process that involves several reaction steps and by-products (for example, NO_2, NO, N_2O, and N_2).[52] **Figure 1d** depicts an electrochemical cell including NO_3RR at the TM SAC cathode and the OER at the anode. Then, we explored the pathway from NO_3^- to NH_3 to understand the entire NO_3RR process. NO is adsorbed on the catalytic active site through various adsorption structures based on the pathways provided in the previous study.[23,53] Thus, the ammonia synthesis routes of NO_3RR are classified as O-end, O-side, N-end, and N-side (**Figure 2**). The pathway for producing the by-product N_2 from NO dimers is also considered, as seen in the lower shaded portion of **Figure 2**. We chose the route with the strongest adsorption of various NO adsorption modes for the subsequent calculation and analysis of the reaction pathways. Thus, we examined the NO_3RR performance of TM SAC systematically via high-throughput calculations, and the performance criterion is the limiting potential ($U_L = -G_{max}/e$, where G_{max} is the highest value of free energy change in all fundamental steps). **Figure 3a** shows that the U_L value in the center of each period is lower than that in the left and rightmost ones, demonstrating that they are potential NO_3RR electrocatalysts to produce NH_3. The volcano diagram between the limiting potential U_L and ΔG^*_{NO3} of different TM SAC catalysts is shown in **Figure 3b**, where Os SAC and Fe SAC are almost located at the top of

the volcano. ΔG^*_{NO3} is chosen as the descriptor, thus, neither too strong nor too weak NO_3^- adsorption energy is beneficial to the completion of the entire reaction; in particular, too weak NO_3^- adsorption inhibits the creation of NOH or NHO (*NO + H^+ + e^- → *NOH/*NHO), whereas too strong adsorption leads to difficult reaction pathway for the formation of NH_3 (*NH_2 + H+ e^- → *NH_3), which is consistent with earlier studies.[45,23] In addition, the final desorption of ammonia is also an important indicator for evaluating reaction activity.[35] Then, we summarized the Gibbs free energy of NH_3 desorption ($\Delta G^*_{NH3-des}$) on various TM SAC catalysts, as shown in **Figure 3c**. The $\Delta G^*_{NH3-des}$ values are all positive except for Cr SAC and Mn SAC, and the promising Os SAC and Fe SAC exhibit the $\Delta G^*_{NH3-des}$ of 0.34 and 0.01 eV, respectively, indicating that they can release from the active aites spontaneously. This scenario is easier than the previously reported NH_3 desorption in the literature (0.96 and 1.08 eV for Ti/g-CN and Zr/g-CN; 0.77 eV for Ru/g-C_3N_4), which promotes the release of active sites, thereby improving catalytic activity. The above results demonstrate that both Os SAC and Fe SAC are desirable electrocatalysts for NO_3RR to produce NH_3; this finding is consistent with the experimental report indicating that Fe SAC exhibits excellent NO_3RR activity.[48]

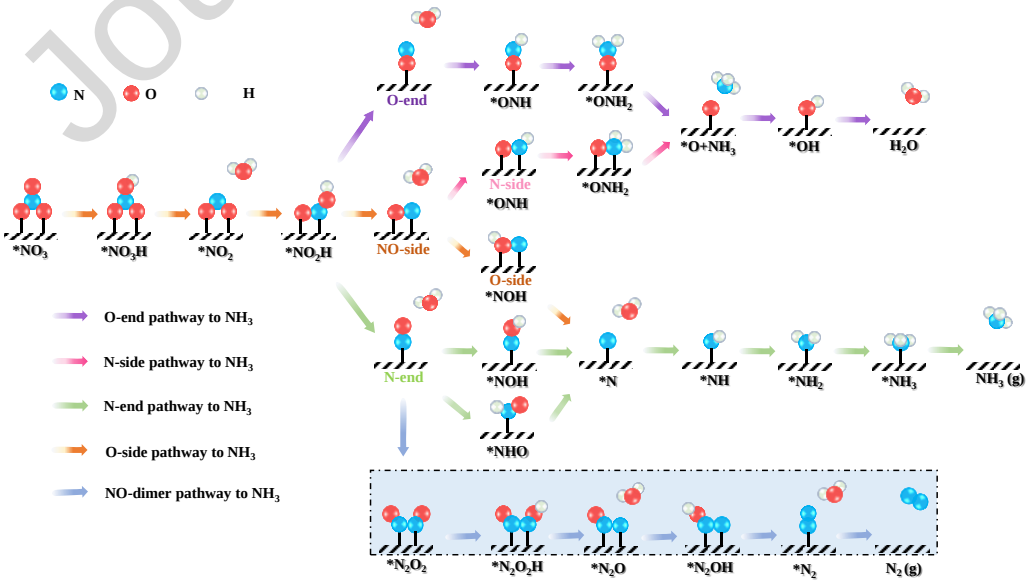

Figure 2. Detailed pathways of NO_3RR, including O-end, O-side, N-end, and N-side pathways to NH_3, as well as NO-dimer pathway to N_2.

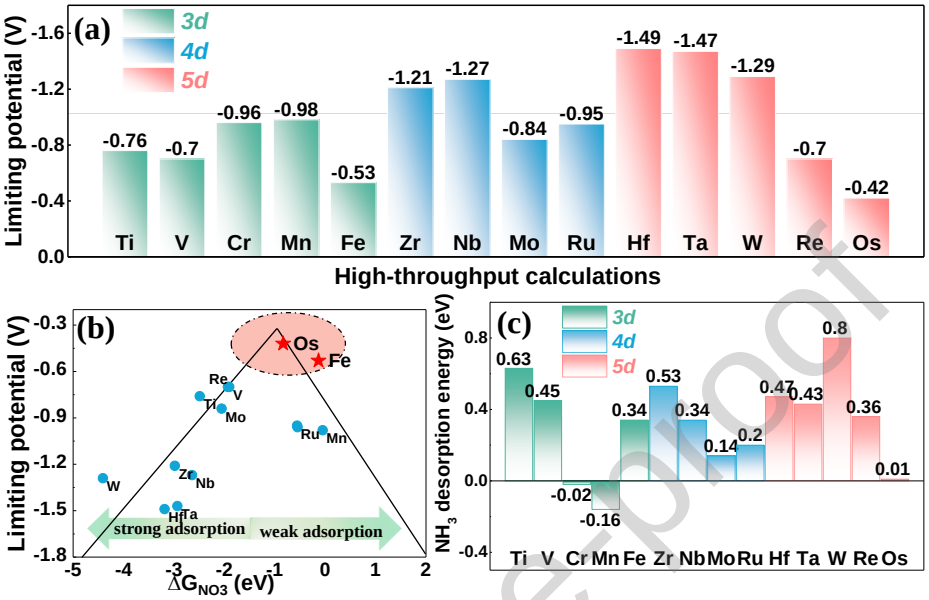

Figure 3. a) Summary of limiting potentials on TM SAC after screening for NO_3RR via the most favorable pathway. b) NO_3RR volcano plot of TM SAC with a descriptor of ΔG^*_{NO3}, where Os SAC and Fe SAC are almost located at the top of the volcano. c) Summarized Gibbs free energy of NH_3 desorption ($\Delta G^*_{NH3\text{-}des}$) on various TM SAC catalysts.

NO_3RR Performance of Fe SAC and Os SAC

The step-by-step free energy diagrams of NO_3RR on Fe SAC and Os SAC presented in **Figures 4a** and **4b** are further investigated to confirm their nitrate-to-ammonia performance. **Figures 4c** and **4d** illustrate the optimal structures of each intermediate product for NH_3 synthesis adsorbed on Fe SAC and Os SAC substrates (the intermediates producing N_2 are shown in **Figure S6**), and the distance between the adsorbed intermediate atom and the metal atom is listed in **Table S2**. For the Fe SAC in **Figure 4a**, NO_3^- is firstly adsorbed on Fe SAC with the free energy slightly increased by 0.01 eV. Subsequently, $*NO_3^-$ is hydrogenated by ($H^+ + e^-$) pair to form $*NO_3H$ intermediate, which is a slightly uphill step

Journal Pre-proof

with the free energy increased by 0.23 eV. Then, the free energy change suddenly dropped by −1.67 eV to form *NO_2. The hydrogenation process is then proceeded to generate *NO_2H through an exothermal process. Following this, *NO_2H is attacked by a (H^+ + e^-) pair, releasing H_2O, whereas *NO stays adsorbed with the Fe-N bond. The change in the free energy profile is −1.62 eV. Next, the free energy of the endothermic process from *NO to *NHO increases by 0.53 eV. In the following steps (*NHO → *N), H proton consecutively attacks *NHO, and the corresponding energy increases by 0.13 eV. In the subsequent steps (*N−*NH−*NH_2−*NH_3), H proton consecutively attacks intermediates, and the corresponding energies drop by −0.35, −1.33, and −0.58 eV. The energy of 0.34 eV is eventually required during the desorption of NH_3. For Os SAC in **Figure 4b**, NO_3^- is spontaneously adsorbed on the active site with a negative ΔG^*_{NH3} of −0.57 eV. Then, it goes through the entire exothermal process until *N is formed with energy changes of −0.68, −0.95, −0.30, −0.76. −0.49, and −1.53 eV in each step. In the following three hydrogenation steps (*N → *NH → *NH_2 →*NH_3), only *N → *NH and *NH_2 →*NH_3 are upward, and their Gibbs free energy changes are 0.42 and 0.33 eV, respectively. The final process is the release of the adsorbed NH_3 with only 0.01 eV free energy changes. The formation of by-products of both Fe SAC and Os SAC, such as NO_2, NO, and N_2, during the entire reaction process is relatively difficult, as shown in **Figure S7** (the corresponding energies increase by 2.42, 2.27, and 0.52 eV for Os SAC and 1.66, 2.71, and 0.77 eV for Fe SAC); so it can be reasonably inferred that the final synthesis of NH_3 can be achieved, which is consistent with recent experimental results.[48] Therefore, the potential determination step (PDS) of Os SAC for the NO_3RR to ammonia is *N → *NH with the value of 0.42 eV, whereas the PDS of Fe SAC is *NO → *NHO with the value of 0.53 eV. The competitiveness of the hydrogen precipitation reaction (HER) must be also considered to verify the selectivity of Fe SAC and Os SAC.

Journal Pre-proof

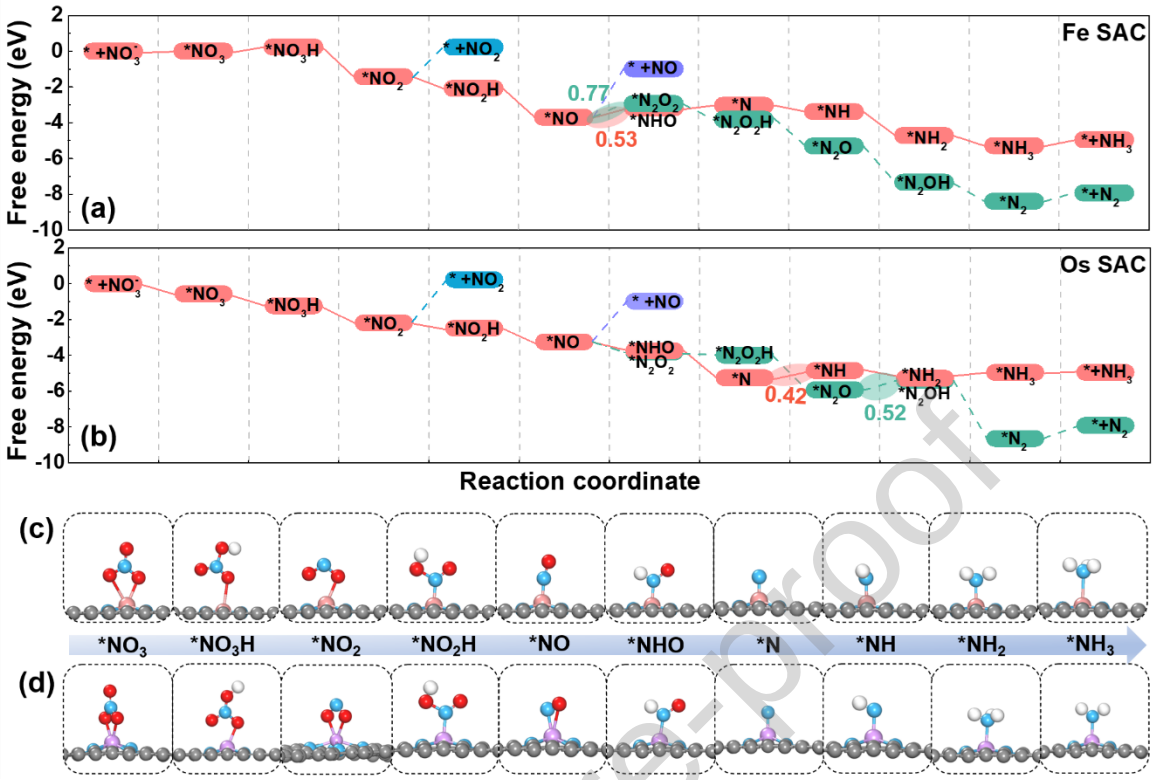

Figure 4. a, b) NO_3RR free energy diagrams of the ideal Fe SAC and Os SAC pathways, respectively. For comparison, the paths for releasing NO_2, NO, N_2O, and N_2 are also displayed. c, d) Structures of NO_3RR intermediates adsorbed on Fe SAC and Os SAC, respectively.

The schematic in **Figure 5a** illustrates that catalysts with excellent selectivity must satisfy the condition that the adsorption energy of NO_3^- (G_{*NO3}) is more negative than that of hydrogen (G_{*H}) to suppress HER, thereby favoring the whole reaction of NO_3RR.[54] Generally, in the acidic solution, the overall HER pathway is:

$H^+ + e^- \rightarrow *H$ (Volmer step), followed by

$*H + H^+ + e^- \rightarrow H_2$ (Heyrovsky step)

or

Journal Pre-proof

*H + *H → H_2 (Tafel step)

where * refers to a potential active site. The free energy diagram for the overall HER process is normally a three-state one, comprising of an initial-state (H^+ + e^-), an intermediate-state of H adsorbed on the catalyst surface (*H), and a final-state product represented by ½H_2.[55] Typically, *H is the key factor to enable favorable HER process and we use G_{*H} to determine the HER performance. **Figure 5b** shows that the G_{*H} can be referred to as Eqs. S7 and S8. The G_{*NO3} of Fe SAC is −0.13 eV, which is higher than G_{*H} (−0.15 eV). This finding indicates that Fe SAC prefers to produce H_2. However, the G_{*NO3} of Os SAC is −0.83 eV, which is more negative than G_{*H} (−0.74 eV). This observation further confirms that Os SAC performs poorly in HER. In summary, the above results indicate that Os SAC has high selectivity for NO_3RR to ammonia.

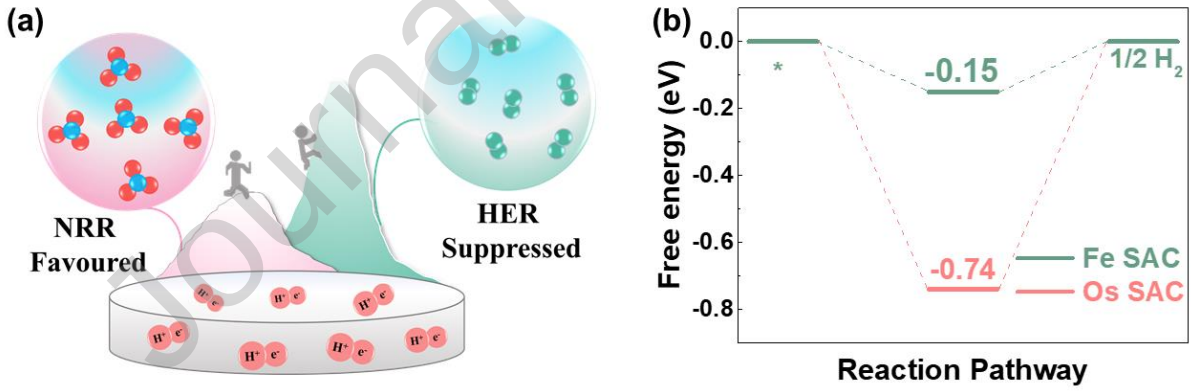

Figure 5. a) Schematic of TM SAC with better selectivity for NO_3RR than HER. b) Gibbs free energy changes for hydrogen reduction reaction on Fe SAC and Os SAC.

NO_3RR Activity Origin on Fe SAC and Os SAC

The first NO_3^- adsorption is the most crucial step in determining NO_3RR. As mentioned above, neither too strong nor too weak NO_3^- adsorption is conducive to the

subsequent reaction. In order to shed light on the origin of NO_3RR activity, we revealed the adsorption of NO_3^- on Os SAC from two aspects, where Fe SAC is chosen as the comparison. First, we calculated the charge density difference to indicate the charge transfer effect between NO_3^- and the substrate. An obvious charge transfer between TM SAC and the adsorbed NO_3^- can be observed in **Figures 6a** and **6b**. The charge transfer from TM atom to NO_3^- (1.28 and 1.43 e^- for Fe SAC and Os SAC, respectively) provides substantial evidence regarding NO_3^- adsorption (−0.13 and −0.83 eV for Fe SAC and Os SAC, respectively), that is, the strong adsorption corresponding to the increasing charge transfer from TM atom to NO_3^-. Moreover, the N–O bond length in the adsorbed NO_3^- ($d_{N-O} = 1.27/1.31$ Å for Fe SAC and $d_{N-O} = 1.32/1.32$ Å for Os SAC) is considerably longer than that in the HNO_3 (gas, d_{N-O}=1.21Å). The increased N–O bond length and electron transfer revealed that the adsorbed NO_3^- on Fe SAC and Os SAC is sufficiently activated. In other words, the more the number of electrons transferred from the catalyst, the more obvious the change of N-O bond length, and the better the activation of $*NO_3$. The electrons transferred by Os SAC are more than those transferred by Fe SAC. Thus, the performance of Os SAC for NO_3^- activation and subsequent NO_3RR activity and selectivity is better than that of Fe SAC. Second, the calculated partial density of states (PDOS) of the two candidates was further evaluated, as shown in **Figures 6c** and **6d**. The PDOS were plotted for the same energy window from −5 eV to 5 eV to facilitate comparison. Our results indicate that on Fe SAC, the 2p states of adsorbed NO_3^- species are delocalized and weakly hybridized with Fe 3d levels throughout a narrow energy range of 4.73 eV to 0 eV. By contrast, the hybridization of the Os SAC substrate and NO_3^- is substantially strong in a wide region between −1.98 and 4.14 eV. The presence of the pronounced hybridization on Os SAC further implies that its interaction with NO_3^- species is too strong, resulting in a low limiting potential.

Journal Pre-proof

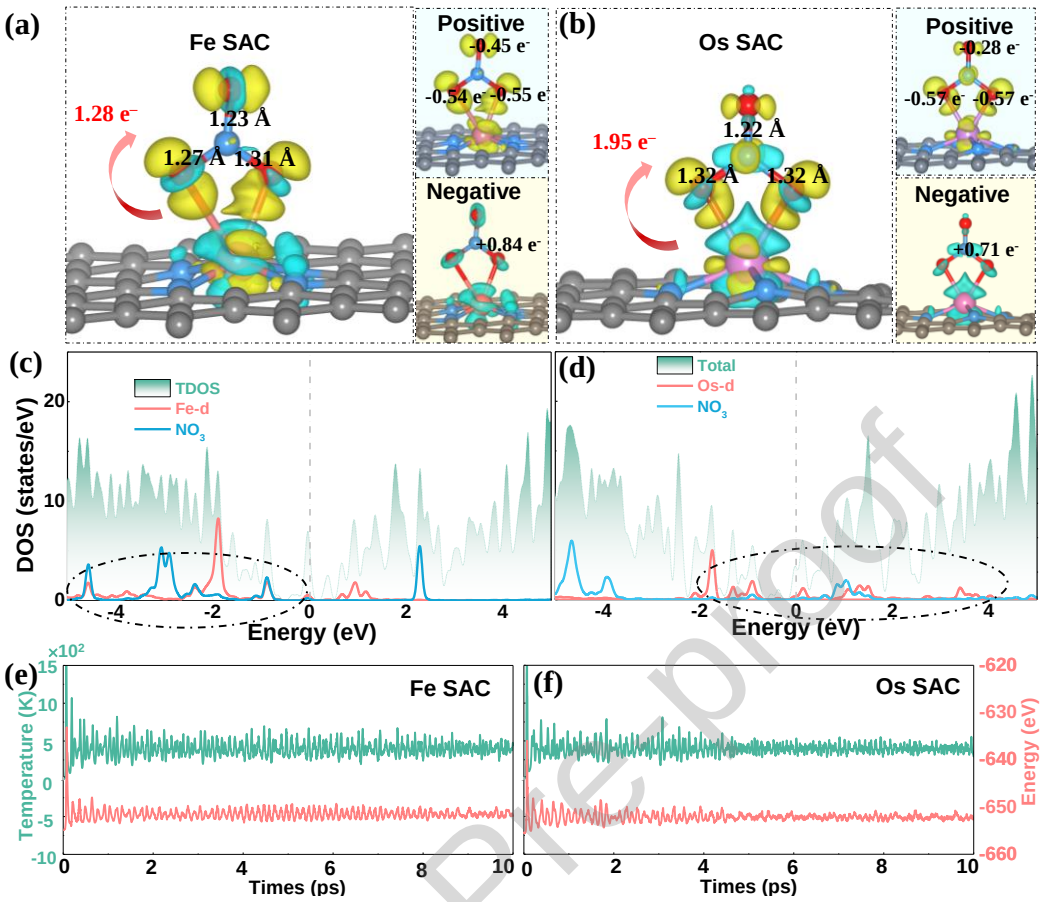

Figure 6. a,b) Charge density differences of NO_3^- adsorbed on Fe SAC and Os SAC. Isosurfaces are 5 × 10^{-3} Å/bohr^3. c,d). PDOS of NO_3^- adsorbed on Fe SAC and Os SAC, respectively. e,f) Energy and temperature evolution versus the AIMD time for Fe SAC and Os SAC, respectively. The AIMD simulation lasts for 10 ps at 500 K.

Stability of Fe SAC and Os SAC

Material stability is an essential condition for researching catalytic characteristics. Thus, the stability of Fe SAC and Os SAC is considered by calculating the ab initio molecular dynamics (AIMD), as shown in **Figures 6e** and **6f**. The completely optimized models of Fe SAC and Os SAC are shown in **Figure S8**. The structure of Fe SAC and Os SAC is still stable after the AIMD evolved by 10,000 steps at the step length of 1 fs. No bond break exists, and the acceptable surface deformation, which oscillates around the original

Journal Pre-proof

configuration, is only little. It also possesses extraordinarily high thermal stability at 500 K. Fe SAC has been successfully synthesized through experiments; hence, Os SAC also has good experimental feasibility in the reaction environment and tremendous promise as a catalyst from NO_3RR to NH_3.

Conclusion

In summary, we studied the activity and selectivity of a series of TM-doped nitrogen-coordinated SACs for electrocatalytic reduction of nitrate to ammonia through high-throughput first-principle calculations. We calculated different reaction paths and compared them with the energy barriers of the by-products by considering the four-step screening method and the various adsorption methods of NO. The results indicated that Fe SAC and Os SAC are located near the top of the volcano plot and have excellent limiting potentials of −0.42 and −0.53 V, respectively. In addition, the energy barriers for the formation of by-products, such as NO_2, NO, N_2O, and N_2, are comparatively large. This finding also demonstrated that Fe SAC and Os SAC have good selectivity for NH_3 formation. Further calculation also illustrated that the selectivity of Os SAC against the side reaction of HER is better than that of Fe SAC. Os SAC also maintains structural stability at 500 K. Therefore, our theoretical analyses confirmed that Os SAC is a potential NO_3RR electrocatalyst with excellent activity, selectivity, and stability, thereby opening new avenues for efficient nitrate degradation and ammonia production, which can decreases the time and economic cost of trial and error in the NO_3RR experimental study. In the future, we will also design and develop more efficient NO_3RR electrocatalysts, such as metallophthalocyanine- and metalloporphyrin-based COFs materials, which will be the focus of our research due to their well-defined crystalline porous structures together with tailored functionalities.

Acknowledgements

Journal Pre-proof

This work was funded by the Science and Technology Development Fund, Macau SAR (File no. 0041/2019/A1, 0046/2019/AFJ, 0021/2019/AIR, 0007/2021/AGJ), University of Macau (File no. MYRG2017-00216-FST, MYRG2018-00192-IAPME, MYRG2020-00187-IAPME), the UEA funding, Science and Technology Program of Guangzhou (2019050001), and National Key Research and Development Program of China (2019YFE0198000). F. Chen acknowledges the Pearl River Talent Program (2019QN01L951). The DFT calculations are performed at High Performance Computing Cluster (HPCC) of Information and Communication Technology Office (ICTO) at University of Macau.

Journal Pre-proof

References

[1] Gruber, N., and Galloway, J. N., An Earth-system perspective of the global nitrogen cycle. Nature 451 (7176) (2008), 293-296

[2] Galloway, J. N., Aber, J. D., Erisman, J. W., Seitzinger, S. P., Howarth, R. W., Cowling, E. B., Cosby, B. J., The nitrogen cascade. 53 (2003), 341-356

[3] Wei, L., Liu, D.-J., Rosales, B. A., Evans, J. W., Vela, J., Mild and Selective Hydrogenation of Nitrate to Ammonia in the Absence of Noble Metals. ACS Catal. 10 (6) (2020), 3618-3628

[4] Foster, S. L., Bakovic, S. I. P., Duda, R. D., Maheshwari, S., Milton, R. D., Minteer, S. D., Janik, M. J., Renner, J. N., Greenlee, L. F., Catalysts for nitrogen reduction to ammonia. Nat. Catal. 1 (7) (2018), 490-500

[5] Reyter, D., Bélanger, D., Roué, L., Study of the electroreduction of nitrate on copper in alkaline solution. Electrochim. Acta 53 (20) (2008), 5977-5984

[6] Su, L., Han, D., Zhu, G., Xu, H., Luo, W., Wang, L.-J., Jiang, W., Dong, A., Yang, J. J. N. l., Tailoring the assembly of iron nanoparticles in carbon microspheres toward high performance electrocatalytic denitrification. Nano lett. 19 (8) (2019), 5423–5430

[7] Tang, C., and Qiao, S.-Z., How to explore ambient electrocatalytic nitrogen reduction reliably and insightfully. Chem. Soc. Rev. 48 (12) (2019), 3166-3180

[8] Jia, R., Wang, Y., Wang, C., Ling, Y., Yu, Y., Zhang, B., Boosting selective nitrate electroreduction to ammonium by constructing oxygen vacancies in TiO2. ACS Catal. 10 (6) (2020), 3533-3540

[9] Xu, S., Ashley, D. C., Kwon, H.-Y., Ware, G. R., Chen, C.-H., Losovyj, Y., Gao, X., Jakubikova, E., Smith, Jeremy M., A flexible, redox-active macrocycle enables the electrocatalytic reduction of nitrate to ammonia by a cobalt complex. Chem. Sci. 9 (22) (2018), 4950-4958

[10] Rosca, V., Duca, M., de Groot, M. T., Koper, M. T. M., Nitrogen Cycle Electrocatalysis. Chem. Rev. 109 (6) (2009), 2209-2244

[11] Service, R. F., New recipe produces ammonia from air, water, and sunlight. Science 345 (6197) (2014), 610-610

[12] Song, Z., Liu, Y., Zhao, J., Zhong, Y., Qin, L., Guo, Q., Geng, Z., Zeng, J., Promoting N2 electroreduction into NH3 over porous carbon by introducing oxygen-containing groups. Chem. Eng. J. 434 (2022), 134636

[13] Zhang, G., Sewell, C. D., Zhang, P., Mi, H., Lin, Z., Nanostructured photocatalysts for nitrogen fixation. Nano Energy 71 (2020), 104645

[14] Zhu, D., Zhang, L., Ruther, R. E., Hamers, R. J., Photo-illuminated diamond as a solid-state source of solvated electrons in water for nitrogen reduction. Nat. Mater. 12 (9) (2013), 836-841

[15] Guo, C., Ran, J., Vasileff, A., Qiao, S.-Z., Rational design of electrocatalysts and photo(electro)catalysts for nitrogen reduction to ammonia (NH3) under ambient conditions. Energ. Environ. Sci. 11 (1) (2018), 45-56

[16]Kitano, M., Inoue, Y., Yamazaki, Y., Hayashi, F., Kanbara, S., Matsuishi, S., Yokoyama, T., Kim, S. W., Hara, M., Hosono, H., Ammonia synthesis using a stable electride as an electron donor and reversible hydrogen store. Nat. Chem. 4 (11) (2012), 934-940

[17] Soloveichik, G., Electrochemical synthesis of ammonia as a potential alternative to the Haber–Bosch process. Nat. Catal. 2 (5) (2019), 377-380

[18] Suryanto, B. H. R., Du, H.-L., Wang, D., Chen, J., Simonov, A. N., MacFarlane, D. R., Challenges and prospects in the catalysis of electroreduction of nitrogen to ammonia. Nat. Catal. 2 (4) (2019), 290-296

[19] Chen, M., Wang, H., Zhao, Y., Luo, W., Li, L., Bian, Z., Wang, L., Jiang, W., Yang, J., Achieving high-performance nitrate electrocatalysis with PdCu nanoparticles confined in nitrogen-doped carbon coralline. Nanoscale 10 (40) (2018), 19023-19030

Journal Pre-proof

[20] Gao, J., Jiang, B., Ni, C., Qi, Y., Zhang, Y., Oturan, N., Oturan, M. A., Non-precious Co3O4-TiO2/Ti cathode based electrocatalytic nitrate reduction: Preparation, performance and mechanism. Appl. Catal. B: Environ. 254 (2019), 391-402

[21] Garcia-Segura, S., Lanzarini-Lopes, M., Hristovski, K., Westerhoff, P., Electrocatalytic reduction of nitrate: Fundamentals to full-scale water treatment applications. Appl. Catal. B: Environ. 236 (2018), 546-568

[22] Martínez, J., Ortiz, A., Ortiz, I., State-of-the-art and perspectives of the catalytic and electrocatalytic reduction of aqueous nitrates. Appl. Catal. B: Environ. 207 (2017), 42-59

[23] Niu, H., Zhang, Z. F., Wang, X. T., Wan, X. H., Shao, C., Guo, Y. Z., Theoretical Insights into the Mechanism of Selective Nitrate-to-Ammonia Electroreduction on Single-Atom Catalysts. Adv. Funct. Mater. 2008533 (2020), 1-8

[24] Wang, Y., Yu, Y., Jia, R., Zhang, C., Zhang, B., Electrochemical synthesis of nitric acid from air and ammonia through waste utilization. Natl. Sci. Rev. 6 (4) (2019), 730-738

[25] Talib, S. H., Yu, X., Yu, Q., Baskaran, S., Li, J. J. S. C. M., Non-noble metal single-atom catalysts with phosphotungstic acid (PTA) support: A theoretical study of ethylene epoxidation. Sci. China Mater. 63 (2020), 1003-1014

[26] Yang, X. F., Wang, A., Qiao, B., Li, J., Liu, J., Zhang, T., Single-atom catalysts: a new frontier in heterogeneous catalysis. Acc. Chem. Res. 46 (8) (2013), 1740-1748

[27] Yu, X., Tian, X., Wang, S., Adsorption of Ni, Pd, Pt, Cu, Ag and Au on the Fe3O4(111) surface. Surf. Sci. 628 (2014), 141-147

[28] Geng, Z., Liu, Y., Kong, X., Li, P., Li, K., Liu, Z., Du, J., Shu, M., Si, R., Zeng, J., Achieving a Record-High Yield Rate of 120.9 for N2 Electrochemical Reduction over Ru Single-Atom Catalysts. Adv. Mater. 30 (40) (2018), 1803498

[29] Guo, H., Li, L., Wang, X., Yao, G., Yu, H., Tian, Z., Li, B., Chen, L., Theoretical Investigation on the Single Transition-Metal Atom-Decorated Defective MoS2 for Electrocatalytic Ammonia Synthesis. ACS Appl. Mater. Inter. 11 (40) (2019), 36506-36514

[30] Kong, Y., Liu, D., Ai, H., Lo, K. H., Wang, S., Pan, H., Theoretical Screening of Single Atoms Supported on Two-Dimensional Nb2CN2 for Nitrogen Fixation. ACS Applied Nano Materials 3 (11) (2020), 11274-11281

[31] Li, L., Wang, X., Guo, H., Yao, G., Yu, H., Tian, Z., Li, B., Chen, L., Theoretical Screening of Single Transition Metal Atoms Embedded in MXene Defects as Superior Electrocatalyst of Nitrogen Reduction Reaction. Small Methods 3 (11) (2019)

Journal Pre-proof

[32] Liang, H.-W., Brüller, S., Dong, R., Zhang, J., Feng, X., Müllen, K., Molecular metal–Nx centres in porous carbon for electrocatalytic hydrogen evolution. Nat. Commun. 6 (1) (2015), 7992

[33] Qiao, B., Wang, A., Yang, X., Allard, L. F., Jiang, Z., Cui, Y., Liu, J., Li, J., Zhang, T., Single-atom catalysis of CO oxidation using Pt1/FeOx. Nat. Chem. 3 (8) (2011), 634-641

[34] Wang, A., Li, J., Zhang, T., Heterogeneous single-atom catalysis. Nat. Rev. Chem. 2 (6) (2018), 65-81

[35] Wang, S., Li, L., San Hui, K., Bin, F., Zhou, W., Fan, X., Zalnezhad, E., Li, J., Hui, K. N., Computational Screening of Single Atoms Anchored on Defective Mo2CO2 MXene Nanosheet as Efficient Electrocatalysts for the Synthesis of Ammonia. Adv. Eng. Mater. (2021)

[36] Yan, Y., Liang, S., Wang, X., Zhang, M., Hao, S. M., Cui, X., Li, Z., Lin, Z., Robust wrinkled MoS(2)/N-C bifunctional electrocatalysts interfaced with single Fe atoms for wearable zinc-air batteries. Proc. Natl. Acad. Sci. 118 (40) (2021)

[37] Ran, N., Song, E., Wang, Y., Zhou, Y., Liu, J., Dynamic coordination transformation of active sites in single-atom MoS2 catalysts for boosted oxygen evolution catalysis. Energy Environ. Sci. 15 (5) (2022), 2071-2083

[38] Zhou, X., Han, K., Li, K., Pan, J., Wang, X., Shi, W., Song, S., Zhang, H., Dual-Site Single-Atom Catalysts with High Performance for Three-Way Catalysis. Adv. Mater. n/a (n/a) (2022), 2201859

[39] Zhuang, Z., Li, Y., Yu, R., Xia, L., Yang, J., Lang, Z., Zhu, J., Huang, J., Wang, J., Wang, Y., Fan, L., Wu, J., Zhao, Y., Wang, D., Li, Y., Reversely trapping atoms from a perovskite surface for high-performance and durable fuel cell cathodes. Nat. Catal. 5 (4) (2022), 300-310

[40] Cui, X., Gao, L., Ma, R., Wei, Z., Lu, C.-H., Li, Z., Yang, Y., Pyrolysis-free covalent organic framework-based materials for efficient oxygen electrocatalysis. J. Mater. Chem. A 9 (37) (2021), 20985-21004

[41] Cui, X., Lei, S., Wang, A. C., Gao, L., Zhang, Q., Yang, Y., Lin, Z., Emerging covalent organic frameworks tailored materials for electrocatalysis. Nano Energy 70 (2020), 104525

[42] Zhang, Z., Wang, W., Wang, X., Zhang, L., Cheng, C., Liu, X., Ladder-type π-conjugated metallophthalocyanine covalent organic frameworks with boosted oxygen

Journal Pre-proof

reduction reaction activity and durability for zinc-air batteries. Chem. Eng. J. 435 (2022), 133872

[43] Liu, C., Li, H., Liu, F., Chen, J., Yu, Z., Yuan, Z., Wang, C., Zheng, H., Henkelman, G., Wei, L., Chen, Y., Intrinsic Activity of Metal Centers in Metal–Nitrogen–Carbon Single-Atom Catalysts for Hydrogen Peroxide Synthesis. J. Am. Chem. Soc. 142 (52) (2020), 21861-21871

[44] Zhu, T., Chen, Q., Liao, P., Duan, W., Liang, S., Yan, Z., Feng, C., Single-Atom Cu Catalysts for Enhanced Electrocatalytic Nitrate Reduction with Significant Alleviation of Nitrite Production. Small 16 (49) (2020), 2004526

[45] Lv, L., Shen, Y., Liu, J., Meng, X., Gao, X., Zhou, M., Zhang, Y., Gong, D., Zheng, Y., Zhou, Z., Computational Screening of High Activity and Selectivity TM/g-C3N4 Single-Atom Catalysts for Electrocatalytic Reduction of Nitrates to Ammonia. J. Phys. Chem. Lett. 12 (45) (2021), 11143-11150

[46] Yang, M., Wang, Z., Jiao, D., Li, G., Cai, Q., Zhao, J., Tuning single metal atoms anchored on graphdiyne for highly efficient and selective nitrate electroreduction to ammonia under aqueous environments: A computational study. Appl. Surf. Sci. 592 (2022)

[47] Guo, S., Heck, K., Kasiraju, S., Qian, H., Zhao, Z., Grabow, L. C., Miller, J. T., Wong, M. S., Insights into Nitrate Reduction over Indium-Decorated Palladium Nanoparticle Catalysts. ACS Catal. 8 (1) (2017), 503-515

[48] Wu, Z. Y., Karamad, M., Yong, X., Huang, Q., Cullen, D. A., Zhu, P., Xia, C., Xiao, Q., Shakouri, M., Chen, F. Y., Kim, J. Y. T., Xia, Y., Heck, K., Hu, Y., Wong, M. S., Li, Q., Gates, I., Siahrostami, S., Wang, H., Electrochemical ammonia synthesis via nitrate reduction on Fe single atom catalyst. Nat. Commun. 12 (1) (2021), 2870

[49] Fei, H., Dong, J., Chen, D., Hu, T., Duan, X., Shakir, I., Huang, Y., Duan, X., Single atom electrocatalysts supported on graphene or graphene-like carbons. Chem. Soc. Rev. 48 (20) (2019), 5207-5241

[50] Chun-Xiang Huang, S.-Y. L., Cong Li1, Bin Peng, Guoliang Li, and Li-Ming Yang, Single-atom catalysts based on two-dimensional metalloporphyrin monolayers for ammonia synthesis under ambient conditions. Nano Res. 10.1007/s12274-021-4009-4 (2021)

Journal Pre-proof

[51] Niu, H., Zhang, Z., Wang, X., Wan, X., Shao, C., Guo, Y., Theoretical Insights into the Mechanism of Selective Nitrate-to-Ammonia Electroreduction on Single-Atom Catalysts. Adv. Funct. Mater. 31 (11) (2020)

[52] Dima, G. E., Beltramo, G. L., Koper, M. T. M., Nitrate reduction on single-crystal platinum electrodes. Electrochim. Acta 50 (21) (2005), 4318-4326

[53] Wang, Y., Xu, A., Wang, Z., Huang, L., Li, J., Li, F., Wicks, J., Luo, M., Nam, D.-H., Tan, C.-S., Ding, Y., Wu, J., Lum, Y., Dinh, C.-T., Sinton, D., Zheng, G., Sargent, E. H., Enhanced Nitrate-to-Ammonia Activity on Copper–Nickel Alloys via Tuning of Intermediate Adsorption. J. Am. Chem. Soc. 142 (12) (2020), 5702-5708

[54] Jasin Arachchige, L., Xu, Y., Dai, Z., Zhang, X., Wang, F., Sun, C., Theoretical Investigation of Single and Double Transition Metals Anchored on Graphyne Monolayer for Nitrogen Reduction Reaction. J. Phys. Chem. C 124 (28) (2020), 15295-15301

[55] Norskov, J. K., Bligaard, T., Logadottir, A., Kitchin, J. R., Chen, J. G., Pandelov, S., Trends in the exchange current for hydrogen evolution. J. Electrochem. Soc. 152 (3) (2005), J23-J26

Journal Pre-proof

Biographies

The information of each author

Shuo Wang received her B.S degree in Materials Science and Engineering from Shenyang Ligong university in 2016 and M.S. degree in 2019 from Department of Chemistry,

Liaoning University. She is currently a Ph.D. candidate at Institute of Applied Physics and Materials Engineering, University of Macau. Her research mainly focuses on the single atom catalysts for the catalytic conversion process and design of novel functional materials by first principle calculation simulation.

Haixing Gao received his B.S degree (2015) and M.S. degree (2018) in Materials and Chemical Engineering from Hainan University. He is currently a Ph.D. candidate at the Institute of Applied Physics and Materials Engineering, University of Macau. His research mainly focuses on the design and synthesis of single-atom site catalysts for the catalytic conversion process.

Journal Pre-proof

Lei Li received his B.S degree in 2017 from Department of Materials and Chemistry and Chemical Engineering, Chengdu University of Technology, and M.S. degree in 2020 from Department of Materials and Energy, University of Electronic Science and Technology of China. Now, he is a Ph.D. candidate at University of Science and Technology of China. His topics are the theoretical prediction and design of new energy materials and catalysts.

Kwan San Hui is a Reader in Mechanical Engineering of School of Engineering, University of East Anglia. He obtained his Ph.D. degree in mechanical engineering at the Hong Kong University of Science and Technology (2008). His research focuses on advanced materials for energy storage, conversion and electrocatalysis.

Journal Pre-proof

Duc Anh Dinh received his PhD degree in the field of Chemistry of Materials at Italian Institute of Technology and Genova University, Italy in 2018. Currently, he is a researcher, working at Nguyen Tat Thanh hi-Tech Institute, Nguyen Tat Thanh University Vietnam. His research interest is focusing in two fields: (1) production and processing of graphene and related two dimensional materials for energy storage, sensors and electronic devices; (2) synthesis and characterization of biodegrade polymers.

Shuxing Wu received his PhD degree inSchool of Materials Science and Engineering at the Pusan National University inSouth Korea in 2018. Then, he joined the Energy and Chemical Engineering Facultyat the Guangdong University of Technology in Guangzhou City. His current research interestsfocus on electrochemical energy storage and spent lithium ion battery recycling.

Journal Pre-proof

Sachin Kumar is a postdoctoral researcher at Yeungnam University, Gyeongsan in South Korea. He received his Ph.D. in 2016 from Motilal Nehru National Institute of Technology, Allahabad, India. He has also worked as a postdoctoral researcher at Shenzhen University, Shenzhen, China and Chonbuk National University, Jeonju, South Korea. He has published more than 30 research articles in highly reputable journals. Presently, his research interests include the development of advanced functional materials for energy storage devices.

Fuming Chen is a Professor at South China Normal University. He received his Ph.D. from the Nanyang Technological University at Singapore in 2011. His current research interests are focused on advanced functional materials for electrochemical energy storage and desalination.

Journal Pre-proof

Zongping Shao is a John Curtin Distinguished Professor at Curtin University, Australia, and also a Professor at Nanjing Tech University, China. He obtained his Ph.D. from Dalian Institute of Chemical Physics, China, in 2000. He worked as a Visiting Scholar at Institut de Researches Sur La Catalyse, CNRS, France, and then a Postdoctoral Fellow at California Institute of Technology, USA, from 2000 to 2005. His current research interests include fuel cells, lithium-ion batteries, metal-air batteries, solar cells, and oxygen-permeable membranes. He has been recognized as a Highly-Cited Researcher by Clarivate Analytics since 2017.

Kwun Nam Hui is an Associate Professor of the Institute of Applied Physics and Materials Engineering, University of Macau. He obtained his Ph.D. degree from The

Journal Pre-proof

University of Hong Kong (2009). His research focuses on electrochemical energy storage and conversion.

CRediT authorship contribution statement

Shuo Wang carried out the theoretical calculations and wrote the manuscript. **Shuo Wang** and **Haixing Gao** contribute equally. **Lei Li**, **Kwan San Hui**, **Zongping Shao**, **Kwun Nam Hui** conceived the idea writing-review & editing. **Duc Anh Dinh**, **Shuxing Wu**, **Sachin Kumar** and **Fuming Chen** contributed to the methodology and project design. All authors were involved in the analysis and discussion of the results.

Declaration of interests

☒The authors declare that they have no known competing financial interests or personal relationships that could have appeared to influence the work reported in this paper.

☐The authors declare the following financial interests/personal relationships which may be considered as potential competing interests:

Graphical abstract

Journal Pre-proof

Abstract

Highlights

- A comprehensive screening of TM SAC candidates for stability, NO_3^- adsorption strength, catalytic activity and selectivity via high-throughput DFT calculations.
- Os SAC exhibited an outstanding performance with a low overpotential of only 0.42 V.
- The increasing charge transfer from TM atom to NO_3^- lead to the strong hybridization of the Os SAC substrate and NO_3^-, then improve the catalytic performance.

Journal Pre-proof